Multi-scale aspects of wave-equation reflection tomography

Maarten V. de Hoop, Purdue University, Robert D. van der Hilst, MIT and Peng Shen, Total*

SUMMARY

In wave-equation reflection tomography, the finite frequency content of data leads to interference effects in the process of medium reconstruction, which are ignored in traditional ray theoretical implementations. We consider inverse scattering of body waves to develop a method of wave-equation migration velocity analysis. We follow a frequency-domain implementation, and emphasize the multi-scale aspects underlying the velocity estimation.

INTRODUCTION

We discuss a method of wave-equation reflection tomography or migration velocity analysis. We use a frequency domain formulation. Wave-equation reflection tomography considers the entire field (without the need to identify individual arrivals, though some time windowing or other processing should be applied to isolate single scattered phases). It involves the application of *annihilators* to the data; (wavefield) annihilators are operators whose action on the wavefield vanishes if the wavespeed model predicts the observations used. In this sense, successful annihilation yields an acceptable estimate of medium wavespeeds. The annihilator-based approach to wave-equation reflection tomography (or to MVA) is akin to differential semblance. The annihilation criterion has significant advantages over conventional mismatch criteria: it handles the effects of scattering in the subsurface; it also enables the efficient exploitation of the inherent 'redundancy' in the scattered wavefield. Using the generalized screen expansion for one-way wave propagation, we find the Fréchet (or sensitivity) kernel associated with the annihilation criterion, and show how it is evaluated with an adjoint state method. We cast the reflection tomography into an optimization procedure; the kernel appears in the gradient of this procedure. We emphasize the multi-scale aspects in a numerical example.

DIRECTIONAL WAVEFIELD DECOMPOSITION

In our method for wave-equation reflection tomography the measure for selecting acceptable models is the successful annihilation of the observed wavefield. In our implementation, the annihilator action is carried out on image gathers at selected depths in a model. Image gathers are formed with the aid of an angle transform applied to downward continued data. To obtain downward continued data from the observed wave field, we use a framework for the decomposition into up and down-going waves.

We carry out directional wavefield decomposition for wave propagation in a smooth background model; subsequently, we combine this decomposition with a formulation that models the scattering of waves off reflectors superimposed on the background. Instead of time t, we make depth z the evolution parameter for wave propagation and data continuation. The remaining (horizontal) coordinates are collected in x. The partial derivatives are denoted by $D_{x_{1,\dots,n-1}} = -\mathrm{i}\partial_{x_{1,\dots,n-1}}$, $D_z = -\mathrm{i}\partial_z$, $D_t = -\mathrm{i}\partial_t$ so that their Fourier domain counterparts become multiplications by $\xi_{1,\dots,n-1}$ (horizontal wave vector), ζ (vertical wave vector) and ω (frequency). An alternative notation for the wave vector used in the seismic literature is (k_x, k_z) for (ξ, ζ).

The system of one-way wave equations

Let u satisfy the wave equation with source term f. In the propagating regime – with D and U denoting the down- and upward propagating constituents of the wavefield, respectively – operator matrices $\mathsf{Q}(z) = \mathsf{Q}(x,z,D_x,D_t)$ can be constructed such that

$$\begin{pmatrix} u_{\mathrm{D}} \\ u_{\mathrm{U}} \end{pmatrix} = \mathsf{Q}(z) \begin{pmatrix} u \\ \frac{\partial u}{\partial z} \end{pmatrix}, \qquad \begin{pmatrix} f_{\mathrm{D}} \\ f_{\mathrm{U}} \end{pmatrix} = \mathsf{Q}(z) \begin{pmatrix} 0 \\ f \end{pmatrix},$$

satisfy the one-way wave equations (Stolk and De Hoop (2005))

$$\left(\tfrac{\partial}{\partial z} + \mathrm{i}B_{\mathrm{D}}(x,z,D_x,D_t)\right) u_{\mathrm{D}} = f_{\mathrm{D}}, \ \left(\tfrac{\partial}{\partial z} - \mathrm{i}B_{\mathrm{U}}(x,z,D_x,D_t)\right) u_{\mathrm{U}} = f_{\mathrm{U}}. \tag{1}$$

In the propagating wave regime, the operator B (= B_{U} or B_{D}) admits an integral representation of the type

$$(Bu)(x,t,z) = (2\pi)^{-n} \int\int\int\int b(x',z,\xi,\omega) \exp[\mathrm{i}\xi(x-x')] \exp[\mathrm{i}\omega(t-t')]\, u(x',t',z)\, \mathrm{d}x'\mathrm{d}t'\,\mathrm{d}\xi\,\mathrm{d}\omega\,, \tag{2}$$

where $b(x',z,\xi,\omega)$ is known in the mathematics literature as the symbol of operator B. The symbol determines the operator, but because it is a smooth function on phase space it is better suited for manipulations such as taking the wavespeed derivatives needed below than the operator itself. For high frequencies the symbol reduces to what is called the principal symbol. We will denote the principal symbol of B from now on by b. It follows that $b = b(x,z,\xi,\omega) = \omega\sqrt{\frac{1}{c_0(x,z)2} - \omega^{-2}\|\xi\|^2}$.

We normalize operator $\mathsf{Q}(z)$, in the propagating regime, such that (1) is selfadjoint; thus

$$\mathsf{Q}(z) = \tfrac{1}{2} \begin{pmatrix} (Q_{\mathrm{D}}^*)^{-1} & -\mathscr{H}Q_{\mathrm{D}} \\ (Q_{\mathrm{U}}^*)^{-1} & \mathscr{H}Q_{\mathrm{U}} \end{pmatrix}, \tag{3}$$

in which * denotes the adjoint, $\mathscr{H}$ denotes the Hilbert transform in time, and $Q_{\mathrm{D,U}} = Q_{\mathrm{D,U}}(z) = Q_{\mathrm{D,U}}(x,z,D_x,D_t)$ are operators with principal symbols $\left(\frac{\omega 2}{c_0(x,z)2} - \|\xi\|^2\right)^{-1/4}$.

A solution for the inhomogeneous equation (1) can be written as

$$u_{\mathrm{U}}(x,t,z) = \int_z^\infty \int\int (G_{\mathrm{U}}(z,z_0))(x,t-t_0,x_0) f_{\mathrm{U}}(x_0,t_0,z_0)\mathrm{d}x_0\mathrm{d}t_0\,\mathrm{d}z_0\,. \tag{4}$$

Here, the Green's function $(G_{\mathrm{U}}(z,z_0))$ is the kernel of propagator $G_{\mathrm{U}}(z,z_0)$; the *adjoint* $G_{\mathrm{U}}(z,z_0)^*$ describes downward propagation from z to z_0 of (1) or upward from z_0 to z in reversed time.

Generalized screen expansion: Perturbation

For the optimization underlying our reflection tomography we need to know the (Fréchet) derivatives of the above mentioned square-root operators with respect to the background wavespeed $c_0(x,z)$. We take this derivative by expanding b into a sum of symbols each of which allows a separation of the phase-space variables (x,ξ). This applies where b is smooth as a function of (x,ξ), which is the case in the propagating regime (or, more general, away from horizontal propagation (when $\omega^{-1}\|\xi\| = c_0^{-1}$)). For computational efficiency, we seek a frequency domain formulation. Such a formulation allows a multi-frequency strategy for optimization.

The expansion mentioned above falls in the category of generalized screen expansions. One way of arriving at a generalized screen expansion is by choosing a reference medium with a wavespeed γ_0 that depends on depth z only. In the process of model updating to be developed below, we assume that at any particular depth z, $\gamma_0(z)$ is the largest lower bound on the wavespeed at that depth according to any of

the allowable models. With this requirement, b is expanded in terms of positive contrasts $[c_0(x,z)^{-2}-\gamma_0(z)^{-2}]$ with c_0 representing the actual wavespeeds in the medium; thus, the c_0 used in the tomography still depends on all n space variables.

The single-square-root operator. The generalized screen expansion of b up to order N is of the form

$$b(x,z,\xi,\omega)=\sum_{j=0}^{N}A_j(\xi,\omega,z)\,S_j[c_0](x,z)\;, \tag{5}$$

with $A_0(\xi,\omega,z)=\omega\sqrt{\frac{1}{\gamma_0(z)2}-\omega^{-2}\|\xi\|^2}$ and $S_0[c_0](x,z)=1$ (cf. (Le Rousseau and De Hoop, 2001, (16))).

Substituting b as in (5) into (2) shows that the single-square-root operator $B_{\rm U}$ in (1) acts on the upgoing wave field $u_{\rm U}$ as

$$(B_{\rm U}u_{\rm U})(x,t,z)\sim F^{-1}_{\omega\to t}\sum_{j=0}^{N}F^{-1}_{\xi\to x}A_j(\xi,\omega,z)$$
$$F_{x'\to\xi}S_j[c_0](x',z)F_{t'\to\omega}u_{\rm U}(x',t',z),\;F^{-1}_{\omega\to t}\hat{B}_{\rm U}=B_{\rm U}F^{-1}_{\omega\to t}, \tag{6}$$

where F denotes the Fourier transform; the frequency domain is indicated by $\hat{}$.

The perturbed single-square-root operator. For the later application of tomography, we consider how $B_{\rm U}$ is perturbed under a smooth perturbation $\delta c_0(x,z)$ of c_0 subject to the constraint that $\gamma_0=\gamma_0(z)$ is kept fixed. (In principle, any perturbation in $\gamma_0(z)$ can be absorbed in $\delta c_0(x,z)$, but for fixed N the accuracy of the propagator depends on $\delta c_0(x,z)$ and may suffer from keeping $\gamma_0(z)$ fixed.) In view of (6) we have

$$(\delta\hat{B}_{\rm U})\hat{u}_{\rm U}(x,\omega,z)\sim\sum_{j=1}^{N}F^{-1}_{\xi\to x}A_j(\xi,\omega,z)F_{x'\to\xi}\,\delta S_j(x',z)\hat{u}_{\rm U}(x',\omega,z)\;. \tag{7}$$

The perturbation δS_j in S_j is expressed in terms of Fréchet derivatives S_j' * as the multiplication

$$\delta S_j(x,z)=S_j'[c_0](x,z)\,\delta c_0(x,z)\;. \tag{8}$$

Substituting (8) into (7) gives the integral operator

$$\hat{B}'_{\rm U}(\hat{u}_{\rm U})\cdot\sim\sum_{j=1}^{N}F^{-1}_{\xi\to x}A_j(\xi,\omega,z)F_{x'\to\xi}S_j'(x',z)\,\hat{u}_{\rm U}(x',\omega,z)\,\cdot_{(x',z)} \tag{9}$$

such that $(\delta\hat{B}_{\rm U})\hat{u}_{\rm U}\sim\hat{B}'_{\rm U}(\hat{u}_{\rm U})\,\delta c_0$. Equation (9) shows how the field $\hat{u}_{\rm U}$ is absorbed as a factor in the screen function, $S_j'\hat{u}_{\rm U}$; the $\cdot_{(x',z)}$ notation reveals that the function (to be inserted at $\cdot$) on which the derivative $\hat{B}'_{\rm U}$ acts, depends on (x',z).

For the purpose of tomography (that is, the adjoint state calculation to obtain an image), we will also need the *adjoint* $\hat{B}'_{\rm U}(\hat{u}_{\rm U})^*$ of $\hat{B}'_{\rm U}(\hat{u}_{\rm U})$. Since $(F_{x\to\xi})^*=F^{-1}_{\xi\to x}$ (up to factors of 2π), we have

$$\hat{B}'_{\rm U}(\hat{u}_{\rm U})^*\cdot\sim\sum_{j=1}^{N}\overline{\hat{u}_{\rm U}(x',\omega,z)}S_j'(x',z)F^{-1}_{\xi\to x'}A_j(\xi,\omega,z)F_{x\to\xi}\;\cdot_{(x,\omega,z)}, \tag{10}$$

with the property that

$$\langle\hat{B}'_{\rm U}(\hat{u}_{\rm U})\delta c_0,\hat{v}\rangle_{(x)}=\langle\delta c_0,\hat{B}'_{\rm U}(\hat{u}_{\rm U})^*\hat{v}\rangle_{(x)}\;\text{ for given } z \text{ and } \omega,$$

where $\langle..,.\rangle$ indicates the inner product in the space of complex, square-integrable functions (the subscript in parentheses indicates the integration variable); $\hat{v}$ represents a trial function of x and ω (and z).

*Here, $S_j'(x,z)=j[c_0(x,z)^{-2}-\gamma_0(z)^{-2}]^{j-1}(-2)c_0(x,z)^{-3}$, $j=1,2,\ldots$. It is natural to absorb the factors j and -2 in A_j and relabel $j:=j-1$.

DATA CONTINUATION IN DEPTH

Upward continuation and modelling of reflection data

We assume wavefield scattering off a contrast δc that contains the singular variations in medium wavepeed. The total medium wavespeed follows the decomposition (subject to $\delta c^{-2}\simeq-2c_0^{-3}\,\delta c$)

$$c^{-2}(x,z)=\gamma_0^{-2}(z)+[c_0^{-2}(x,z)-\gamma_0^{-2}(z)]-2c_0^{-3}(x,z)\,\delta c(x,z)\;.$$

To obtain a downward/upward continuation representation of the single-scattered waves, we introduce the extended medium contrast,

$$\mathsf{R}(s',r',t',z')=\tfrac{1}{2}\,\delta(t')\delta(r'-s')(c_0^{-3}\delta c)(\tfrac{r'+s'}{2},z')\;; \tag{11}$$

one can view R as a data-like representation of the contrast. Let $d(s,r,t)=Q^*_{{\rm U},s}(0)Q^*_{{\rm U},r}(0)u(s,r,t,z=0)$ ($Q_{{\rm U},s}(z)$ is short for $Q_{\rm U}(s,z,D_s,D_t)$ and $Q_{{\rm U},r}(z)$ is short for $Q_{\rm U}(r,z,D_r,D_t)$); $u=u(s,r,t,z)$ represents (decomposed) seismic data as a function of time, generated at depth z below the surface by fictituous sources s and observed by fictituous receivers r (which is sometimes referred to as a 'sunken survey'):

$$u(s,r,t,z)=\int_z^\infty(H(z,z')Q_{{\rm U},s}(z')Q_{{\rm U},r}(z')\,D_t^2\mathsf{R}(.,z'))(s,r,t)\,{\rm d}z',$$
$$(H(z,z'))(s,r,t,s',r',t')=$$
$$\int_{\rm IR}(G_{\rm U}(z,z'))(s,t-t'-\bar{t},s',0)(G_{\rm U}(z,z'))(r,\bar{t},r',0)\,{\rm d}\bar{t}. \tag{12}$$

Then, u solves an inhomogeneous double-square-root (DSR) equation

$$(\tfrac{\partial}{\partial z}-{\rm i}C(s,r,z,D_s,D_r,D_t))u=g,$$
$$C(s,r,z,D_s,D_r,D_t)=B_{\rm U}(s,z,D_s,D_t)+B_{\rm U}(r,z,D_r,D_t), \tag{13}$$

in which $g=g(s,r,t,z)=Q_{{\rm U},s}(z)Q_{{\rm U},r}(z)D_t^2\mathsf{R}(.,z)$.

Downward continuation and imaging of reflection data

The *adjoint* operator $H(0,z)^*$ is used to propagate the data backward. We consider

$$\psi d\mapsto\mathsf{D}=H(0,z)^*Q^*_{{\rm U},s}(0)^{-1}Q^*_{{\rm U},r}(0)^{-1}\psi d\;, \tag{14}$$

where ψ is a (source, receiver, and time) taper that suppresses the parts of the data that one does not want to consider in the imaging process. In (14), D is a function of (s,r,t,z); for $t>0$, $\mathsf{D}(s,r,t,z)$ can be identified with $u(s,r,t,z)$ in (13).

An image of δc can be obtained from D by applying imaging conditions: $\mathsf{I}(x,z)=\mathsf{D}(s=x-\frac{h}{2},r=x+\frac{h}{2},t,z)|_{h=0,t=0}$, where we have introduced subsurface horizontal midpoint-offset coordinates, (x,h).

ANGLE TRANSFORM, DATA ANNIHILATORS

We build on the work by Stolk and De Hoop (2001) and De Hoop and Van der Hilst (2003). In the imaging process, the reflection point becomes the image point, and the redundancy in the data becomes manifest in the multiple images that are generated by extracting the different scattering angles and azimuths in this process. This is accomplished by the angle transform. In this transform, we encounter a variable p that is essentially half the difference between the horizontal slowness vectors associated with source and receiver rays at the depth where the transform is applied. The precise relation between p and scattering angle and azimuth can be found in (De Hoop et al., 2003, (88)-(90)). For an acceptable wavespeed model the images are independent of scattering angle and azimuth.

Angle transform and common image-point gathers

With, as before, $u = u(s,r,t,z)$, and h the horizontal offset between r and s, we introduce

$$(Ru)(x,z,p) = \int_{\mathbb{R}^{n-1}} u(x-\tfrac{h}{2},x+\tfrac{h}{2},ph,z)\chi(x,z,h)\,\mathrm{d}h$$
$$= \frac{1}{2\pi}\int\int_{\mathbb{R}^{n-1}} \hat{u}(x-\tfrac{h}{2},x+\tfrac{h}{2},\omega,z)\exp(-\mathrm{i}\omega ph)\,\chi(x,z,h)\,\mathrm{d}h\mathrm{d}\omega,$$

(note the zero intercept time: $t = 0+ph$; see also De Bruin *et al.* (1990)). Here, $h \mapsto \chi(x,z,h)$ is a taper in h with the property that $\chi(x,z,0) = 1$. We apply R to the downward continued data, $\mathsf{D}(s,r,t,z)$ (cf. (14)), to obtain the 'wave-equation' angle transform, $\mathscr{A}$,

$$\mathscr{A}d = RH(0,z)^*Q^*_{\mathrm{U},s}(0)^{-1}Q^*_{\mathrm{U},r}(0)^{-1}\psi d\,. \tag{15}$$

The outcome of this angle transform applied to the data is

$$\bar{\mathsf{I}}(x,z,p) = (\mathscr{A}d)(x,z,p) = (R\mathsf{D})(x,z,p)\,. \tag{16}$$

For each x, $\bar{\mathsf{I}}(x,z,p)$ is a common image-point gather in (z,p). With an appropriate choice of χ the common image-point gathers are free of false events, even in the presence of caustics (Stolk and De Hoop (2001); Stolk et al. (2005)). In Sava et al. (1999) a related but different transform is used. For an acceptable model c_0, $\mathscr{A}$ maps data d to a p-family of reconstructions of δc, and for each p the same image $(\bar{\mathsf{I}}(x,z,p))$ of $\delta c(x,z)$ is obtained (exploiting that the image gathers are free of artifacts).

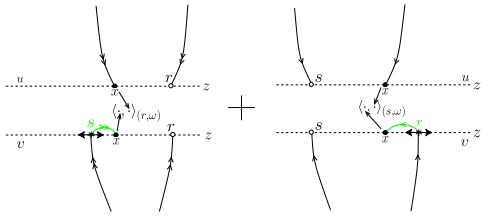

Figure 1: The evaluation of the kernel. The single and double arrows refer to the two terms in between brackets in (24); the gray arrows indicate the generalized screen operations.

Annihilators of the downward continued data

Since the outcome $(\mathscr{A}d)(x,z,p)$ should be independent of p (strictly upon additional amplitude corrections), annihilators of the data follow to be $W_i := \left(\frac{\partial}{\partial t}\right)^{-1}\langle\mathscr{A}^{-1}\rangle\frac{\partial}{\partial p_i}\mathscr{A}$, $i = 1,\ldots,n-1$, where $\langle\mathscr{A}^{-1}\rangle$ indicates a regularized inverse of $\mathscr{A}$: $W_i d = 0$. We consider the annihilators not in the data but in the image domain: $\frac{\partial}{\partial p_i}\mathscr{A}\left(\frac{\partial}{\partial t}\right)^{-1}$, which leads to the introduction of

$$(R'_i u)(x,z,p) = \int_{\mathbb{R}^{n-1}} u(x-\tfrac{h}{2},x+\tfrac{h}{2},ph,z)\,h_i\chi(x,z,h)\,\mathrm{d}h$$
$$= \frac{1}{2\pi}\int\int_{\mathbb{R}^{n-1}} \hat{u}(x-\tfrac{h}{2},x+\tfrac{h}{2},\omega,z)\exp(-\mathrm{i}\omega ph)\,h_i\chi(x,z,h)\,\mathrm{d}h\mathrm{d}\omega.$$

The annihilation of the data is thus replaced by an annihilation, $R'_i\mathsf{D}$, of the set of image gathers $\mathscr{A}d$, $i = 1,\ldots,n-1$, parametrized by p.

For the purpose of tomography, we furthermore need the *adjoint* $(R'_i)^*$ of R'_i. Let I denote a trial image as a function of (x,z,p), then

$$\langle R'_i u,\mathsf{I}\rangle_{(x,p)} = \frac{1}{2\pi}\int\int_{\mathbb{R}^{2n-2}}\hat{u}(s,r,\omega,z)$$
$$\overline{\left(\int_{\mathbb{R}^{n-1}}(r-s)_i\exp[\mathrm{i}\omega p(r-s)]\,\mathsf{I}(\tfrac{1}{2}(s+r),z,p)\mathrm{d}p\right)}$$
$$\chi(\tfrac{1}{2}(s+r),z,r-s)\,\mathrm{d}s\mathrm{d}r\mathrm{d}\omega = \langle\hat{u},(\hat{R}'_i)^*\mathsf{I}\rangle_{(s,r,\omega)} \quad \text{given } z, \tag{17}$$

from which we identify $(\hat{R}'_i)^*$. We note that $(\hat{R}'_i)^*$ yields an extension of a (differentiated) image gather to fictituous data, in the nature of R defined in (11). By removing the factor h_i in the integrand, we immediately obtain an expression for $\hat{R}^*$. By Parseval's theorem, we also find R^*, $(R^*\mathsf{I})(s,r,t,z) = \int_{\mathbb{R}^{n-1}}\delta(t-p(r-s))\mathsf{I}(\frac{1}{2}(s+r),z,p)\mathrm{d}p$, with the property that $\langle Ru,\mathsf{I}\rangle_{(x,p)} = \langle u,R^*\mathsf{I}\rangle_{(s,r,t)}$.

AN OPTIMIZATION PROCEDURE

In our approach to reflection tomography the wavespeed estimation is cast into the minimization of the functional $\mathscr{J}[c_0]$, given by

$$\tfrac{1}{2}\sum_i\int\int|(R'_iH(0,z)^*Q^*_{\mathrm{U},s}(0)^{-1}Q^*_{\mathrm{U},r}(0)^{-1}\psi d)(x,z,p)|^2\mathrm{d}(x,z)\mathrm{d}p\,, \tag{18}$$

where the integration is over all scattering or image points (x,z) and 'angles' p. A standard method for optimization can be invoked to carry out the minimization of $\mathscr{J}$. Here, we derive a method for evaluating the Fréchet kernel or gradient of $\mathscr{J}$. The method for evaluating the gradient of a functional derived from the solution of a partial (or pseudo)differential equation is known as the adjoint state method.

Under a smooth perturbation δc_0 of c_0 subject to the constraint that γ_0 is kept the same, the perturbation of the downward-continued data u is δu; the perturbation of the functional then follows to be $\delta\mathscr{J} = \sum_i\int\int(R'_iu)\,(R'_i\delta u)\,\mathrm{d}(x,z)\mathrm{d}p$, because R' is independent of c_0. Recognizing an inner product in (x,p), it follows that

$$\delta\mathscr{J} = \frac{1}{2\pi}\int\int\int(\sum_i(\hat{R}'_i)^*R'_iu)\,(\overline{\delta\hat{u}})\,\mathrm{d}(s,r)\mathrm{d}z\,\mathrm{d}\omega \tag{19}$$

by definition of the adjoint in (17). The integration over (s,r) is identified as an inner product $\langle.,.\rangle_{(s,r)}$. In view of the complex conjugation we recognize in (19) a time correlation between a 'source' and a 'field'. The field δu satisfies the equation

$$(\tfrac{\partial}{\partial z} - \mathrm{i}\hat{C}(s,r,z,D_s,D_r,\omega))\delta\hat{u} = \mathrm{i}\,\delta\hat{C}(s,r,z,D_s,D_r,\omega)\hat{u} \tag{20}$$

in the single-scattering approximation, where $\delta\hat{C}$ is the perturbation of operator $\hat{C}$ with δc_0, which follows from (7) and (13). Equation (20) is solved in the direction of increasing z (downward) with homogeneous initial conditions at $z = 0$. These conditions follow from the assumption that c_0 is known where the data are measured (that is, near $z = 0$). Equation (20) follows the wavespeed perturbation for the downward continuation of the data, and its solution can be generated by a composition of thin-slab propagators (De Hoop et al. (2003)).

In preparation of the application of the volume integral form of the reciprocity theorem of the time-correlation type in the framework of one-way wave theory, we now distinguish two states: one state with *contrast* source distribution $\mathrm{i}\,\delta\hat{C}u$ and field δu, and one state with *mismatch* source distribution $\sum_i(\hat{R}'_i)^*R'_iu$ and field, say $\hat{v}$. The mismatch source distribution is generated at any image point where full annihilation of a downward continued reflection (R'_iu) has failed. We have

$$(-\tfrac{\partial}{\partial z} + (\mathrm{i}\hat{C}(s,r,z,D_s,D_r,\omega))^*)\hat{v} = \sum_i(\hat{R}'_i)^*R'_iu\,, \tag{21}$$

which is also known as the adjoint field. This equation is solved in the (upward) direction of decreasing z, with vanishing initial condition for some large z (say, at the bottom of the model).

The reciprocity theorem of the time-correlation type, applied to (21)-(20), now implies that we can write (19) in the equivalent form

$$\delta\mathscr{J} = \frac{1}{2\pi}\int\int\hat{v}\,(\overline{\mathrm{i}\,\delta\hat{C}\hat{u}})\,\mathrm{d}(s,r,z)\,\mathrm{d}\omega\,. \tag{22}$$

The frequency integral is kept as the outside integral because the kernel computation is to be carried out in the ω-domain. A scale-decomposition follows upon applying frequency window functions $\hat{\psi}_k$, corresponding with a wavelet transform, to the data. We use that $(R_i'\psi_k)^*$ yields $\hat{\psi}_k(\hat{R}_i')^*$ in the right-hand side of (21), resulting in a solution $\hat{v}_k$ and hence a contribution $\delta\mathscr{J}_k$.

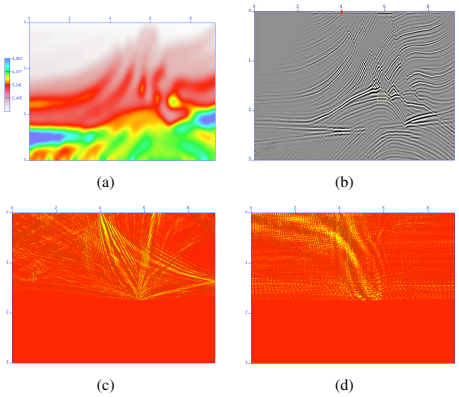

Figure 2: (a): Wavespeed model (c_{true}) used to generate the data. (b): Image obtained by wave-equation migration using the true wavespeed model. (c): The contribution to the gradient (cf. (24)) due to a single reflector inside the marked yellow box and a single source located at the red disk (b), using the entire bandwidth of the data. (d): The contribution to the gradient, but here for low frequencies (3.3-6.6 Hz) only.

We can now combine the concepts developed in the previous sections and formulate the sensitivity kernel. To do this, we write the perturbation $\delta\hat{C}$ in the form of a derivative $\delta\hat{C}\hat{u} = \hat{C}'(\hat{u})\,\delta c_0$. We obtain

$$\frac{1}{2\pi}\int\int \hat{v}(\mathrm{i}\overline{\delta\hat{C}\hat{u}})\,\mathrm{d}(s,r,z)\mathrm{d}\omega = \int \left[(\mathrm{i}C'(u))^*v\right]\,\delta c_0\,\mathrm{d}(x,z) \qquad (23)$$

having inlcuded ψ_k, a partition in frequency. To extract the kernel of the derivative of $\mathscr{J}$ out of (23), we make use of relation (10) with x' playing the role of s or r. Thus, the kernel attains the form

$$\begin{aligned}(\mathrm{i}C'(u))^*v(x,z) = \frac{1}{2\pi}\int \mathrm{d}\omega(-\mathrm{i})\\ \left[\int \hat{B}'_{\mathrm{U},s}(\hat{u})^*\hat{v}\,\mathrm{d}r + \int \hat{B}'_{\mathrm{U},r}(\hat{u})^*\hat{v}\,\mathrm{d}s\right] \sim \frac{1}{\pi}\,\mathrm{Re}\int_0^\infty \mathrm{d}\omega(-\mathrm{i})\\ \sum_{j=0}^{N}\left[\int \overline{\hat{u}(x,r,\omega,z)}\,\underbrace{S_j'(x,z)F_{\sigma\to x}^{-1}A_j(\sigma,\omega,z)F_{s\to\sigma}}\,\hat{v}(.,r,\omega,z)\,\mathrm{d}r\right.\\ \left.+\int \overline{\hat{u}(s,x,\omega,z)}\,\underbrace{S_j'(x,z)F_{\rho\to x}^{-1}A_j(\rho,\omega,z)F_{r\to\rho}}\,\hat{v}(s,.,\omega,z)\,\mathrm{d}s\right]. \qquad (24)\end{aligned}$$

We used the symmetry in frequency to restrict the evaluation to positive values. In (24), we finally use for $\hat{u}$ the downward continued data D (cf. (14)) and for the adjoint field, $\hat{v}$, the solution of (21) in which the mismatch source distribution is evaluated from D. Thus equation (24) is of the form of a time cross correlation of the downward continued data and the adjoint field excited by a mismatch force nested in a generalized screen operation (indicated by underbraces). In fact, the general structure is of the form of solving a couple of **evolution equations**, and subjecting the solutions to a tomographic **imaging operation**. The formulation in the *frequency domain* is amenable to a subsequent multi-scale analysis. The procedure to evaluate (24) is illustrated in figure 1. It consists of the following steps: (i) starting at the top, downward continue the data all the way to the bottom (cf. (14)) while storing the results at all intermediate depths; (ii) starting at the bottom, evaluate the mismatch source from the downward continued data, (iii) upward continue (in the frequency domain) step-by-step the adjoint field (cf. (21)), and (iv), at each depth, evaluate the frequency contribution to the kernel (cf. (24)).

DISCUSSION: MULTI-SCALE BEHAVIOR, AN EXAMPLE

Using synthetic data generated in the Marmousi model, we illustrate here the effectiveness of the angle transform (16), the character of the cost functional used for optimization (18), and the finite-frequency sensitivity kernel (that is, the gradient, (24)) associated with the annihilator-based method for 'wave-equation' reflection tomography. As the background model, we consider a smooth version of Marmousi (figure 2(a)). For reference, in figure 2(b) we show the image. We then evaluate the kernel contribution (a function of (x,z)) for a source (s) indicated by a solid red dot, and a mismatch source ($R_i'u$) restricted to a point on a reflector within the yellow box, see figure 2(c). This figure reveals the complexity of the kernel owing to finite-frequency (interference) effects and multipathing. An imprint of the rays connecting the mismatch source point to the source and a receiver determined by the reflector dip is visible. (N.B. Note also, on the right, the multipathing and reflections at the (computational) boundary. These reflections could be suppressed by appropriate absorbing boundary conditions or PML.) In figure 2(d), we illustrate the contribution to the kernel for low frequencies (3.3-6.6 Hz) only. The multi-frequency decomposition of the kernel reveals the multi-scale aspects of wave-equation migration velocity analysis. We observe how differently, through the wave dynamics, different frequency windows sample the subsurface.

In figure 3 we illustrate the local convexity and smoothness (for an analysis in the context of annihilators, see Stolk and Symes (2003)) of the cost functional by considering a one-parameter family of perturbations, generated by the differential model illustrated in figure 3(a), about the model depicted in figure 2(a).

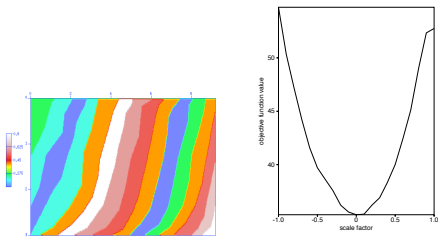

Figure 3: (a) An inhomogeneous wavespeed perturbation, Δc_0. (b) Functional evaluated at $c_0 = \alpha\Delta c_0 + c_{\text{true}}$, where α is a scalar ranging from -0.1 to 0.1, and c_{true} is the true wavespeed model shown in figure 2(a), respectively.

REFERENCES

De Bruin, C., C. Wapenaar, and A. Berkhout, 1990, Angle-dependent reflectivity by means of prestack migration: Geoph., **55**, 1223–1234.

De Hoop, M., J. Le Rousseau, and B. Biondi, 2003, Symplectic structure of wave-equation imaging: A path-integral approach based on the double-square-root equation: Geoph. J. Int., **153**, 52–74.

De Hoop, M. and R. Van der Hilst, 2003, Global wave-equation reflection tomography: Center for Wave Phenomena, **453**.

Le Rousseau, J. and M. De Hoop, 2001, Modeling and imaging with the scalar generalized-screen algorithms in isotropic media: Geoph., **66**, 1551–1568.

Sava, P., B. Biondi, and S. Fomel, 1999, Amplitude-preserved common image gathers by wave-equation migration: 69th Ann. Internat. Mtg., Expanded Abstracts, 824–827.

Stolk, C. and M. De Hoop, 2001, Seismic inverse scattering in the 'wave-equation' approach: MSRI preprint, **#2001-047**.

——— 2005, Modeling of seismic data in the downward continuation approach: SIAM J. Appl. Math., **65**, 1388–1406.

Stolk, C., M. De Hoop, and W. Symes, 2005, Kinematics of shot-geophone migration: Geophysics, **submitted**.

Stolk, C. and W. Symes, 2003, Smooth objective functionals for seismic velocity inversion: Inverse Problems, **19**, 73–89.

EDITED REFERENCES

Note: This reference list is a copy-edited version of the reference list submitted by the author. Reference lists for the 2006 SEG Technical Program Expanded Abstracts have been copy edited so that references provided with the online metadata for each paper will achieve a high degree of linking to cited sources that appear on the Web.

REFERENCES

De Bruin, C., C. Wapenaar, and A. Berkhout, 1990, Angle-dependent reflectivity by means of prestack migration: Geophysics, **55**, 1223–1234.

De Hoop, M., J. Le Rousseau, and B. Biondi, 2003, Symplectic structure of wave-equation imaging: A path-integral approach based on the double-square-root equation: Geophysical Journal International, **153**, 52–74.

De Hoop, M., and R. Van der Hilst, 2003, Global wave-equation reflection tomography: Center for Wave Phenomena, 453.

Le Rousseau, J., and M. De Hoop, 2001, Modeling and imaging with the scalar generalized screen algorithms in isotropic media: Geophysics, **66**, 1551–1568.

Sava, P., B. Biondi, and S. Fomel, 1999, Amplitude-preserved common image gathers by wave-equation migration: 69th Annual International Meeting, SEG, Expanded Abstracts, 824–827.

Stolk, C., and M. De Hoop, 2001, Seismic inverse scattering in the 'wave-equation' approach: MSRI preprint, 2001–047.

———, 2005, Modeling of seismic data in the downward continuation approach: SIAM Journal of Applied Mathematics, **65**, 1388–1406.

Stolk, C., M. De Hoop, and W. Symes, 2005, Kinematics of shot-geophone migration: 75th Annual International Meeting, SEG, Expanded Abstracts, 1866–1869.

Stolk, C., and W. Symes, 2003, Smooth objective functionals for seismic velocity inversion: Inverse Problems, **19**, 73–89.